



# NOVEL STRATEGY FOR WATER SIDED INTERFACIAL 3D3C FLOW-VISUALIZATION USING A SINGLE CAMERA

Björn Voss\*, Christoph S. Garbe\*

\*Image Processing and Modelling (IPM),  
Interdisciplinary Center for Scientific Computing (IWR),  
University of Heidelberg, Germany

## KEYWORDS:

**Main subject(s):** *particle based 3D3C flow field measurement,*

**Fluid:** *interfacial fluid flow,*

**Visualization method(s):** *PSV, bichromatic depth estimation,  
single camera setup*

**Other keywords:** *acceleration measurement, tensor based pattern analysis*

**ABSTRACT :** *Accurate measurements of fluid flow close to the free water-sided air-water interface are vital for a proper understanding and quantification of interfacial transport phenomena. Yet, these measurements are difficult to attain with current PIV or PTV based techniques. Moreover, the observed flow structures are highly turbulent, leading to large out-of-plane components in laser-sheet based approaches.*

*This contribution addresses these issues by introducing a novel particle based visualization technique for three component, three dimensional velocity fields (3C3D) close to the free air-water interface. The major advantage of this technique is that depth measurements are relative to the water surface and in a Lagrangian coordinate frame. Hence, uncertainties due to locating the position of the moving interface are circumvented. Also, accelerations can be deduced directly from our approach, making it an ideal tool for the quantification of interfacial fluid dynamical transport processes.*

## 1 Introduction

### 1.1 Physical Background

Transport processes through the air-water boundary layer play an important role in many industrial applications and in environmental research. The main resistance for the interfacial transport of momentum, heat and gases is dominated by the topmost layer, known as viscous boundary layer. In this layer, diffusion is the dominant transport process. Due to turbulence and coherent flow structures, the viscous boundary layer is disrupted intermittently. For a better understanding of these transport processes, flow measurements in a Lagrangian frame of reference with depth information relative to the interface are an important prerequisite. The proposed method enables measurements in a Lagrangian frame of reference independent of a surface tracking method. Depth information is obtained relative to the water-surface from a special illumination setup in conjunction with image processing procedures.

## 1.2 Particle Based Flow Measurements

Most particle based flow visualization techniques such as *particle image velocimetry* (PIV), *particle tracking velocimetry* (PTV) and *laser speckle velocimetry* (LSV) exploit the difference between two images of the particle seeded water body to extract spatial changes caused by the flow field. In contrast, *particle streak velocimetry* (PSV) uses a single image, recorded with a long exposure time  $\Delta t$  to extract information of the flow-field. In classical PSV approaches, the imaged streak structures which correspond to particle trajectories are used to measure velocities averaged over the exposure time of the imaging device [8]. For an extension of these methods to enable three dimensional (3D) velocity measurements, a common strategy is the use of additional imaging devices. These multi-camera setups provide 3D data in an Eulerian frame of reference. For a detailed review on these techniques we refer to [9] and [2].

The measurement strategy presented in this contribution enhances the traditional PSV measurement by using alternating periodic light sources to code velocity information during the exposure time as an intensity modulation on the streak structure. Additionally, the depth information is measured using a bichromatic method introduced by [4]. This enables the extraction of 3D3C data with a high spatial and temporal resolution in a Lagrangian frame of reference using a single camera.

## 2 Experimental Apparatus and Flow-Feature Extraction

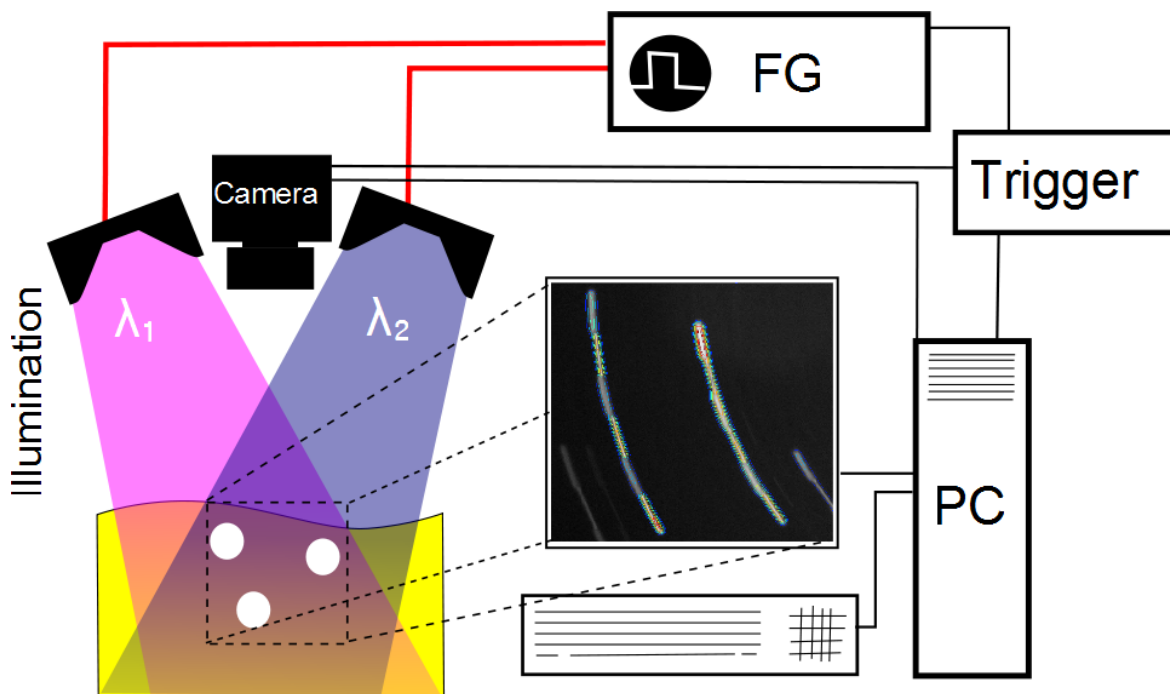


Fig. 1 Single camera setup for the visualization of 3D3C flow-fields. Function-generator (FG), frame-grabber and trigger device are synchronized by a desktop PC with is also used to store the recorded image sequences. The liquid is seeded with small spheres which are imaged as streak, due to the long exposure of the CCD device. The spatial intensity modulation along the streak structures is caused by the alternating two-wavelength illumination and the supplemented dye with a wavelength-dependent absorption characteristic.

### 2.1 Experimental Setup

The measurement setup shown in Fig. 1 consists of a CCD device with 5MPx and a 12bit depth resolution. The fluid is seeded with “Silver-Coated Hollow Ceramic Spheres” [Potters Industry Inc.] ( $\varnothing = 100\mu\text{m}$ ,  $\rho = 1.1 \text{ g/cm}^2$ ). For the illumination two *Light Emitting Diode* (LED) arrays with radiation maxima at  $\lambda_1 = 408\text{nm}$  and  $\lambda_2 = 470\text{nm}$  and a total radiant flux of 6Watts were used. Tartrazine turned out to be a feasible dye for the *bichromatic depth estimation*, because of the large difference in the extinction coefficients at the used wavelengths. The LEDs are controlled by a function-generation (FG) that enables an illumination with arbitrary, periodic signals. The image processing and data acquisition library *heuristic*<sup>®</sup> was used to implement the measurement framework for the synchronization of the whole setup and for image. The image analysis and feature extraction software described later was developed in C++.

## 2.2 Measurement Principle

The major idea of the proposed visualization technique is to combine a two dimensional PSV setup with a *bichromatic depth estimation* technique developed by [4], to obtain 3D3C information from the flow-field near the water surface.

### 2.2.1 Bichromatic Depth Estimation

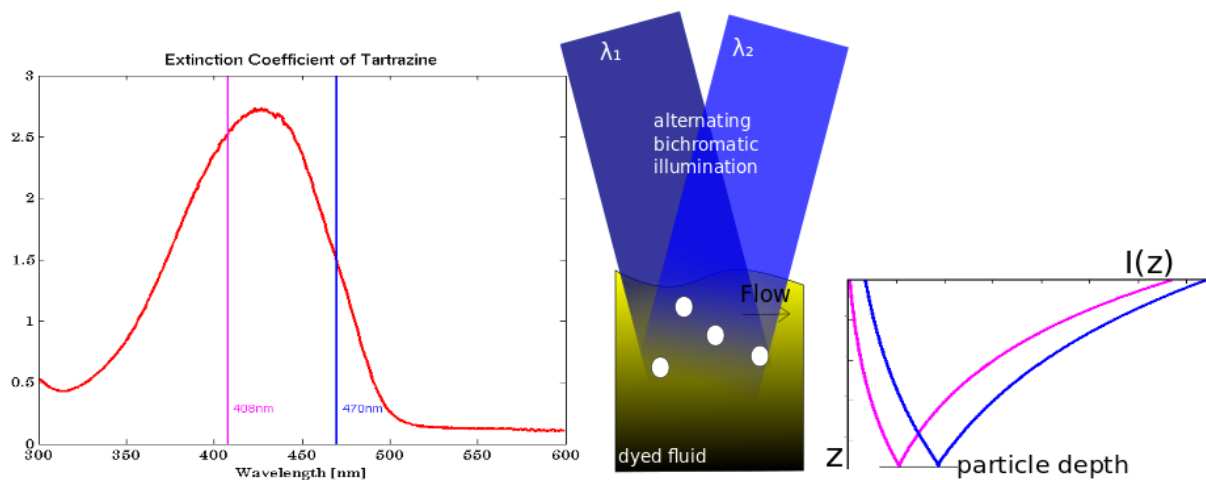


Fig. 2 (left side) Absorption characteristic of the supplemented dye (red line) and the radiation maxima of both used LED arrays  $\lambda_1 = 408\text{nm}$  (violet) and  $\lambda_2 = 470\text{nm}$  (blue); (right side) basic principle of the *bichromatic depth estimation*.

As described by [4], the distance of the seeded spheres to the water surface can be coded by means of a supplemented dye. This dye and the illumination wavelength are chosen in a way that the penetration depth  $z_i^*$  shows a large difference between the used wavelengths. The measured gray value  $g_i(x)$  in the recorded image is given by the Beer-Lambert's law for each wavelength  $\lambda_i \forall i \in \{1,2\}$  for a particle at depth  $z$ :

$$g_i(z) = g_{0i} \exp\left(-\frac{z}{z_i^*}\right) \quad (1)$$

To neglect the signal dependence on the particle size and on spatial inhomogeneities of the illumination, we can compute the particle depth from the ratio of the signals measured for both wavelength according to

$$z(g_{1,2}) = \frac{z_1^* z_2^*}{z_1^* - z_2^*} \left( \ln \left( \frac{g_1}{g_2} \right) + \ln \left( \frac{g_{02}}{g_{01}} \right) \right) \quad (2)$$

Thus,  $z(g_{1,2})$  only depends on the ratio of the reflected intensities, the particle size cancels out and has no influence on the depth estimation.

### 2.2.2 Bichromatic Particle Streak Velocimetry

Traditional PSV measurement strategies use the recorded streak structures to extract kinematic features of the particle movement; i.e., direction, depth, speed and curvature of the particle's trajectory. The temporal resolution of these methods is limited by the exposure time  $\Delta t$ , thus all these features are the result of an averaging over  $\Delta t$ . In order to increase the temporal resolution our proposed method uses a new illumination strategy. To obtain a time series of the previously described kinematic features, two alternating periodic light sources of the same constant frequency  $F$  were used instead of a constant illumination. By this strategy the kinematic features are coded in the intensity pattern for every point on the trajectory. Thus the frequency of the illumination signals  $F$  [Hz] are known as well as the pixel sizes  $\alpha$  [m/px], the instant frequency  $f(x)$  [1/px] of the signal  $g(x)$  can be used to compute instant horizontal velocity  $v_h$  for each point on the streak structure.

$$v_h(x) = \alpha F \frac{1}{f(x)} \quad (3)$$

The horizontal acceleration  $a_h$  can be computed from the first derivative of the instantaneous frequency using:

$$a_h(x) = \alpha F \frac{d}{dx} \frac{1}{f(x)} \quad (4)$$

For the *bichromatic depth estimation*, the particle velocity has to be taken into account, as well. As a result the gray value of a particle at a certain position on the image depends not only on the illumination and the supplemented dye but also on the time it remains at this position. It is obvious that a fast moving particle will yield a lower gray value than a slow one, spreading out the same intensity on a longer streak. This intensity dependence does not influence the depth estimation because the estimated depth is not estimated from total gray values but from the ratio of the two gray values from the different illumination wavelengths. Thus particle depth  $z$  can be computed for the zero crossings of the signal  $g(x)$  on the middle line using the next maximum and minimum of the signal as input for equation (2).

In a further step, the horizontal velocity and the middle line can be used to compute the horizontal particle position  $x_h(t) = (x_1(t), x_2(t))$  for every time point  $t \in (0, \Delta t)$  and the particle depth  $z(t)$  at all zero-crossings of  $g(x)$ .

### 2.3 Streak Pattern Extraction

In order to obtain robust low-level features for the detection of the streak structures in the recorded image, the quadrature-based boundary tensor introduced by [6] is applied to the recorded images. Among other low-level features the boundary tensor enables the computation of the local *boundary strength* and the *local orientation* shown in Fig. (3).

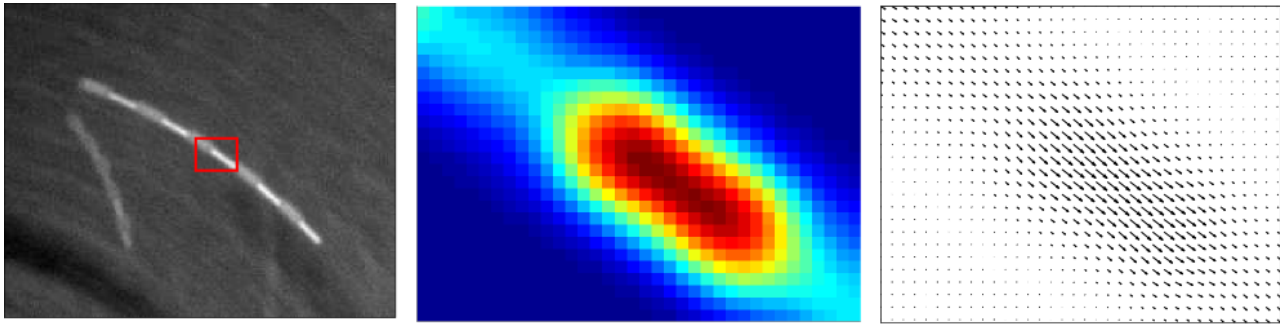


Fig. 3 from left to the right: image data of a particle streak; *local boundary strength* of the area within red box; *local direction* of the area within the red box

The boundary strength represents a non-linear enhancement of linear structures, significantly reducing noise and artifacts in the image. On the basis of these two features, a center-line-extraction algorithm was developed to detect all streak structures and their center-lines (which correspond to the streak trajectories mapped on the image plane) with sub pixel precision.

The iterative extraction routine for the detection of single streaks structures is based on two assumptions. The first is that all streak patterns in an image represent the path of one particle during the integration time  $\Delta t$  and that the exact particle positions lie on the center-line of this structure. The second assumption is that for all streak structures the cross-section perpendicular to the streak direction has a Gaussian profile.

For each streak the algorithm starts at the pixel with the largest *local boundary strength* value and iterates along the streak. In every step the algorithm is fitting a Gaussian bell-curve perpendicular to the structure, and extracts the exact center-line position using the maximum of the bell-curve. This iterative sampling procedure is stopped if the width of the Gaussian bell-curve is above a certain threshold, in which case the algorithm returns to the initial point and iterates along the streak structure in the negative *local direction*. The maxima of the fitted Gaussian bell-curves are assumed to be points on the streaks center-line.

Algorithm:

- (1) Use the boundary tensor to compute the *local boundary strength* and the local orientation
- (2) **Set** the initial pixel position to the pixel with the highest boundary strength
- (3) Initialize a list  $L = \emptyset$ , to store the middle line of the current streak structure
- (4) Extract the intensities on a line perpendicular to the local direction with sub pixel precision using a bilinear interpolation
- (5) Fit a Gaussian bell curve to the values extracted from the line using a Levenberg Marquard fitting routine
- (6) Compute the exact middle line position from the maximum of the bell curve, the local direction and the current pixel position. Add this position to  $L$
- (7) **If** the width of the bell curve is below a threshold go one pixel into direction given by the local direction and then **go to** (4)  
**Else** run steps (4) to (7) a second time with the negative local directions
- (8) **Set** the boundary strength of a local neighborhood around the extracted streak structure to zero.
- (9) **If** the maximum of the boundary strength values is larger than a threshold go to (1) and start the extraction of a new streak structure

## 2.4 Flow-Feature Extraction Using the Hilbert Huang Transform

The recorded intensity path of the extracted streak structures can be seen as a periodic, nonlinear and non-stationary signal. In the flow-feature extraction, the frequency and the amplitude of the intensity signal extracted from the streaks center-line plays an important role. As described above, it is directly related to the particle's horizontal speed and acceleration. In the field of signal processing there is a large number of approaches to handle this kind of signal, which for example, also occur during the processing of audio files, in seismographic measurements or in electrocardiographic measurements. The most common strategy for the analysis and representation of this kind of time series is the fast Fourier transform (FFT) [7]. Thus the observed particles may accelerate or change their depth during one exposure time, the frequency and the amplitude of the observed signal  $g(x)$  may also change along the streak structure. The FFT is futile for the analysis of signals with a time dependent intensity component, thus its result in the frequency domain corresponds to the global average over the whole signal. To overcome this limitation of the FFT, we employ the Hilbert Huang transform [9] (HHT) for the transformation of a measured signal into the frequency domain. In this transformation, the signal is decomposed into a number of basic functions called *intrinsic mode functions* (IMFs) using an *empirical mode decomposition* (EMD) [9]. In contrast to the FFT these basic functions are computed from the time series itself and thus they are unique for each data set. For further processing the IMFs can be divided into three groups: noise, periodic signal and offset. In the next step the Hilbert Transform is used to determine instantaneous frequency  $f(x)$  and the amplitude  $A(x)$  which can be used to compute the horizontal velocity, the horizontal acceleration and the particle depth.

### 2.4.1 Empirical Mode Decomposition

As mentioned above the recorded signals basically contain three modes: (1) a high frequent noise from the image acquisition, (2) a periodic signal which is caused by the alternating periodic illumination and (3) a non-periodic offset, as shown in Fig. 4.

These assumptions are also the major motivation for the EMD, which was introduced for the decomposition of a nonlinear, non-stationary signal into single mode IMFs. These basic functions are simple oscillatory signals that have the same number of extrema and zero-crossings and are symmetric with respect to the local mean. The IMF can be seen as a simple harmonic function, the difference is only that the simple harmonic function has constant amplitude and frequency over time. The EMD itself is an iterative process that consists of a series of siftings. During each iteration the mean of a spline fit through all local maxima and a spline fit through all local minima is subtracted from the signal  $g(x)$ . The process ends if the following two constraints are fulfilled. (1) The number of local extrema and the number of zero-crossings of the resulting signal are equal or differ at most by one. (2) The mean of the spline fitting the maxima and the spline fitting the minima is zero. The resulting signal that fulfills both constraints is the first IMF  $c_1$ . For the computation of higher order IMFs we iteratively compute the residual  $r_i = g(x) - c_i$  and compute the next higher IMF  $c_{i+1}$  from this residual using the previously described iterative shifting process. After  $N$  iterations the residual  $r_N$  is not longer a periodic signal and the complete input signal can be represented by the sum of all IMFs and the non-periodic residual.

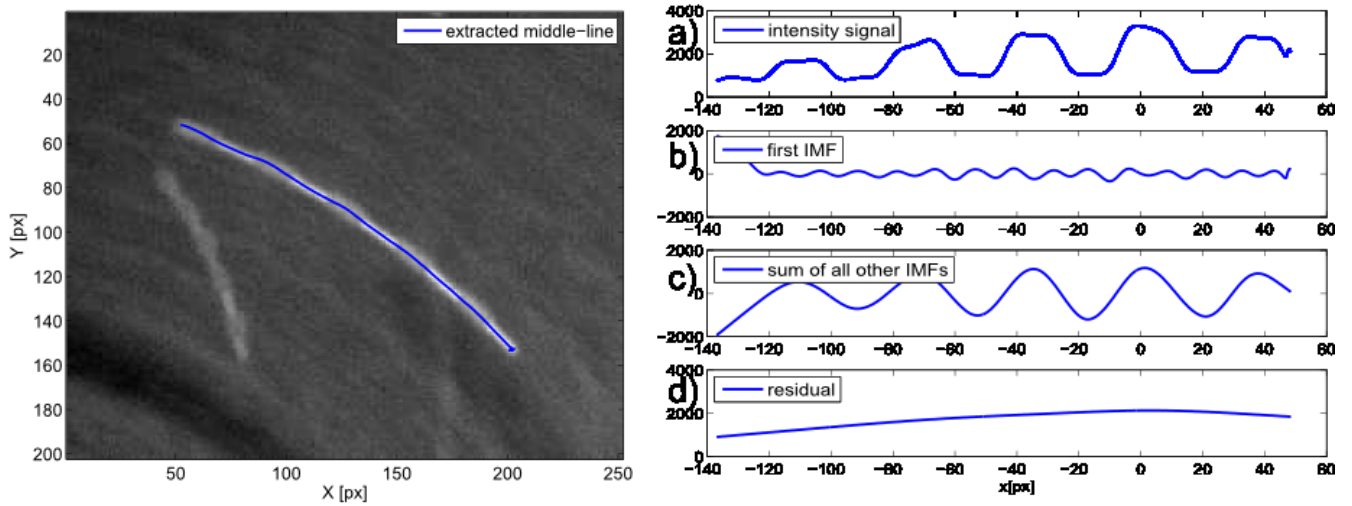


Fig. 4 (left side) Original data with the extracted middle line of the streak structure (blue line), these data were recorded using a box-function for the alternating bichromatic illumination; (right side) EMD decomposition of the signal on the extracted middle line.

### 2.4.2 Hilbert Transform

For the extraction of the instantaneous spatial frequency of the intensity signal on streak patterns, the corresponding complex *strong analytical signal* (SAS)  $g_a(x) = g(x) + i\hat{g}(x)$  is computed using the Hilbert transformed signal [5]

$$\hat{g}(x) = P \frac{1}{\pi} \int_{-\infty}^{+\infty} \frac{g(x')}{x - x'} dx'. \quad (5)$$

With the Cauchy principal value  $P$ . Every SAS can be expressed in the polar form  $g_a(x) = A(x) \exp(i\theta(x))$  in terms of an instantaneous amplitude  $A(x)$  and phase  $\theta(x)$  which can be computed as follows

$$A(x) = \sqrt{g(x)^2 + \hat{g}(x)^2} \quad \text{and} \quad \theta(x) = \arctan\left(\frac{\hat{g}(x)}{g(x)}\right). \quad (6)$$

As a consequence we can determine the instant frequency by computing the spatial phase change  $f(x) = d/dx \theta(x)$ . Using this frequency, the horizontal velocity and acceleration can be computed for each point along the particles trajectory as described in section (2.2.2).

### 2.4.3 Preliminary Results

The evaluation of some first test measurements using the previous described algorithms show very promising results. First measurements suggest that our newly proposed technique is above par with the technique proposed by [4]. We are currently performing extensive accuracy measurements with ground truth data to characterize our approach and to quantify its accuracy under a wide range of conditions. In our preliminary measurements, a rotating water body was used to obtain different velocities in one measurement. The dye concentrations in these measurements were chosen as described in [4] to observe a depth range between 0 and 15mm. Tests with different periodic illumination patterns showed that sinusoidal illumination pattern improve the extraction of the streak patterns. An additional

advantage of the sinusoidal intensity modulation is that it does not contain high frequent modes which complicate the *empirical mode decomposition*.

### 3 Conclusions

This contribution introduces a novel visualization technique for the extraction of interfacial flows in the air-water boundary layer. Simply spoken, it is a combination of PSV measurement extended by an intensity-modulated two-wavelength light source and a *bichromatic depth estimation*. Beside the ability of extracting 3D3C information of the interfacial flow-field in a Lagrangian frame of reference the major advantage is the high temporal resolution. For each recorded tracer particle this framework enables the extraction of the 3D position, the horizontal velocity and their temporal path during the exposure time.

First proof of concept measurement using simple flow fields show very promising results. The accuracy and applicability in a wide range of conditions is currently being analyzed in dedicated ground truth measurements.

### References

1. C.S. Garbe, U. Schimpf, und B. Jähne, "A surface renewal model to analyze infrared image sequences of the ocean surface for the study of air-sea heat and gas exchange," *Journal of Geophysical Research*, vol. 109, 2004.
2. J. Grue, P.L.F. Liu, und G.K. Pedersen, *PIV and water waves*, World Scientific, 2004.
3. N. Huang, Z. Shen, S. Long, M. Wu, H. Shih, Q. Zheng, N. Yen, C. Tung, und H. Liu, "The empirical mode decomposition and the Hilbert spectrum for nonlinear and non-stationary time series analysis," *Proceedings of the Royal Society of London. Series A: Mathematical, Physical and Engineering Sciences*, vol. 454, März. 1998, S. 995, 903.
4. M. Jehle und B. Jähne, "A novel method for three-dimensional three-component analysis of flows close to free water surfaces," *Experiments in Fluids*, vol. 44, März. 2008, S. 469-480.
5. F. King, G. Smethells, G. Helleloid, und P. Pelzl, "Numerical evaluation of Hilbert transforms for oscillatory functions: A convergence accelerator approach," *COMPUTER PHYSICS COMMUNICATIONS*, vol. 145, Mai. 2002, S. 256-266.
6. U. Köthe, "Low-level Feature Detection Using the Boundary Tensor," *Visualization and Processing of Tensor Fields*, Berlin: Springer, 2006, S. 63-79.
7. C. Rader und N. Brenner, "A new principle for fast Fourier transformation," *Acoustics, Speech and Signal Processing, IEEE Transactions on*, vol. 24, Jan. 2003, S. 266, 264.
8. S.K. Sinha und P.S. Kuhlman, "Investigating the use of stereoscopic particle streak velocimetry for estimating the three-dimensional vorticity field," *Experiments in Fluids*, vol. 12, Apr. 1992, S. 377-384.
9. C. Tropea, A.L. Yarin, und J.F. Foss, *Springer handbook of experimental fluid mechanics*, Springer, 2007.

### Copyright Statement

The authors confirm that they, and/or their company or institution, hold copyright on all of the original material included in their paper. They also confirm they have obtained permission, from the copyright holder of any third party material included in their paper, to publish it as part of their paper. The authors grant full permission for the publication and distribution of their paper as part of the ISFV14 proceedings or as individual off-prints from the proceedings.